Modeling and Simulation of Fixed Bed Batch Bark Drying

by

Marcus Huttunen

Department of Chemical Engineering
Lund University

June 2015

Supervisor: André Holmberg
Examiner: Professor Stig Stenström

Postal address
P.O. Box 124
SE-221 00 Lund, Sweden
Web address
www.chemeng.lth.se

Visiting address
Getingevägen 60

Telephone
+46 46-222 82 85
+46 46-222 00 00
Telefax
+46 46-222 45 26

Preface

I would like to thank my supervisor A. Holmberg for providing ideas and inspiration when developing the model. I would also like to thank him for the experimental data that was needed both for designing the isotherm and the data from the pilot plant which was compared with the model.

I would also like to thank M. Lundberg, A. Lövgren and F. Tegner for providing help with Matlab and good company during the master thesis.

Lastly I would like to thank Södra for providing the industrial data that the model was compared with.

Abstract

During this master thesis four variation of a model were created with the goal to simulate the drying process of bark. All four variations were compared with experimental data from a pilot plant and heat and mass transfer coefficient were calibrated against the experimental data.

The four model variations are:

- Adiabatic saturation model
- Heat and mass transfer coefficient model
- Isotherm model
- Fraction model

The adiabatic saturation model was the worst and did not represent the drying curve very well, especially at low moisture contents.

The heat and mass transfer coefficient model represented the drying curve better, especially for birch and pine. But when it came to spruce it was a consistent error between the experimental data and the models drying curve.

The isotherm model did not affect the drying rate very much compared to what was already seen in the heat and mass transfer coefficient model but some changes could be seen at the temperature profiles and for birch, which had the lowest initial moisture content.

The best representation of the drying rate was achieved, with up to 99 % coefficient of determination, with the fraction model that had three size fractions.

The fraction model was lastly compared with industrial data with success.

Sammanfattning

I examensarbetet gjordes fyra variationer av en modell med målet att simulera torkningen av bark. Alla fyra variationerna jämfördes med experimentella data från en pilotanläggning och värme- och massöverföringskoefficienten kalibrerades mot experimentella data.

De fyra modellvariationerna är:

• Adiabatisk mättningsmodell

• Värme och massöverföringskoefficientsmodell

• Isotermmodell

• Fraktionsmodell

Den adiabatiska mättnadsmodellen var det sämsta och representerade inte torkningskurvan mycket bra, särskilt vid låga fukthalter.

Värmen och massöverföringskoefficient modellen representerade torkkurvan bättre, särskilt för björk och tall. Men för gran det var en konsekvent fel mellan de experimentella data och modeller torkkurvan.

Isotermmodellen påverkade inte torkningshastigheten mycket jämfört med vad som redan sett i värmen och massöverföringskoefficienten modell men vissa förändringar kunde ses på temperaturprofilerna och björkens viktkurva, som hade den lägsta initiala fukthalt.

Den bästa representationen av torkningshastigheten uppnåddes, med upp till 99% detemina-tionsskoefficient, med fraktionsmodellen som hade tre storleksfraktioner.

Fraktionsmodellen jämfördes slutligen med industriella data med framgång.

Table Of Contents

1 Introduction

Nowadays bark is mostly used as a fuel in pulp and paper mills. With increasing interest for renewable energy resources and more energy effective processes the interest in optimizing the utilization of bark as a fuel has grown. In this master thesis the possibility to dry bark for a higher energy output has been investigated.

Initially bark has high moisture content, varying from 0.5 kg water/kg dry matter and up to 2.0 kg water/kg dry matter, when stripped of the tree. The goal with drying is to use low value heat, such as low pressure steam or waste heat, to lower the moisture content of the bark and therefore increase the effective heating value. The bark will combust at a temperature much higher than the temperature used for the drying air, the overall process becomes that low temperature heat can be traded for heat at a much higher temperature that can be used for high pressure steam generation.

The aim of this master thesis was to create a model that represents reality, resulting in that the model can be used as a basis when designing industrial scale dryers. Four different models were done and the final model was lastly validated against industrial data from Södra Cell, Värö.

In this master thesis chemical and physical properties behind drying have been first studied in a literature review and with gathered information a model was created to simulate the drying process in Matlab.

The results from the model have been compared to experimental data from a pilot plant that was set up in the apparatus hall in Kemicentrum in Lund. A few different models were tested and fitted to the experimental data by varying the heat and mass transfer coefficients.

2 Literature Review

In order to gather enough knowledge to set up a mathematical model, the physical and chemical properties of bark were studied alongside with the general heat and mass transfer equations for packed beds.

2.1 Drying process

The drying process can be split up into three phases:

- Heating of the fixed bed
- Constant drying rate
- Falling drying rate (non-linear)

2.1.1 Heating of the fixed bed

The first phase is the heating of the fixed bed to the adiabatic saturation temperature. This is under the assumption that the starting temperature of the bed will be lower than adiabatic saturation temperature. During this step limited drying will occur.

2.1.2 Constant drying rate

When the bed has been heated to the adiabatic saturation temperature a linear drying phase will take place as the drying air will reach its equilibrium saturation before leaving the bed.

2.1.3 Falling drying rate

The declining phase starts when the temperature of the drying air leaving the bed starts to increase above the adiabatic saturation temperature which indicates that the air isn't reaching equilibrium anymore. This happens when the desorption isotherm is reached so moisture in the middle of the particle that cannot diffuse to the edge of the particle as fast the air can take up moisture. Therefore the limiting factor will be the diffusion inside the particle. [1], [2]

2.2 Heat & Mass transfer models

In order to determine how fast the bark will dry heat and mass transfer models needs to be set up. These models can be setup as theoretical or semi-empirical models. Below in Equation 2.1 the general form for a semi-empirical model based on Fick's second law can be seen. Usually for these methods the moisture content, u, changes with σa that includes diffusion, thermal conductivity and mass transfer. [1], [3]

$$\frac{du}{dt} = \sigma a(u - u_E) \tag{2.1}$$

In order to get a better description of the problem σa can be split up into two components, σa_1 and σa_2. As seen in Equation 2.2. This method was used later to assign a different mass transfer coefficient for different particle sizes.

$$\frac{du}{dt} = \sigma a_1(u - u_E) + \sigma a_2(u - u_E) \tag{2.2}$$

For theoretical models the general form for the heat and mass transfer is set up. Some simplifications are normally done and for this model the derivatives in all three dimensions won't be needed. Heat transfer in the particle is limited by the heat conductivity according to Equation 2.3, where k is the heat conductivity in respective direction. [4]

$$\rho Cp \frac{\partial T}{\partial t} = \frac{\partial}{\partial x}\left(k_x \frac{\partial T}{\partial x}\right) + \frac{\partial}{\partial y}\left(k_y \frac{\partial T}{\partial y}\right) + \frac{\partial}{\partial z}\left(k_z \frac{\partial T}{\partial z}\right) \quad (2.3)$$

The mass transfer of moisture throughout the particle is limited by the effective diffusion. The effective diffusion, D_{eff}, will differ dependent on direction due to the fiber structure in bark. The difference in moisture content, ∂u, will follow Equation 2.4 below. [4]

$$\frac{\partial u}{\partial t} = \frac{\partial}{\partial x}\left(D_{eff_x} \frac{\partial u}{\partial x}\right) + \frac{\partial}{\partial y}\left(D_{eff_y} \frac{\partial u}{\partial y}\right) + \frac{\partial}{\partial z}\left(D_{eff_z} \frac{\partial u}{\partial z}\right) \quad (2.4)$$

2.3 Dependent variables

Dependent variables are those that have a direct effect on the drying process and below the most important are listed.

Temperature: Higher temperature of the inlet air will be able to dry the bark faster since a higher temperature will transfer more energy to the wet material and therefore evaporate more water and hold a higher partial pressure of the water.[5]

Particle size: If the particles are smaller the linear drying phase will be a larger part of the total drying time. This happens since in smaller particles it will take less time for moist to diffuse from the middle to the edge.

Bark type: Different types of bark will have slightly different properties such as different diffusion coefficients for water and density. As this research has been done aiming to be implemented on a full scale pulp plant the type of wood chosen was the same that is used at the plant, which are spruce, pine and birch. [6] Also experimental data show that different types of bark will have different initial moisture content as they absorb different amounts of water.

Air flow: Air flow rate will naturally increase the drying rate as there will be more air to take up moisture from the bark.

2.4 Physical data

To construct the model data needs to be gathered, data listed below will be estimated, gathered from literature or measured by doing experiments.

- Particle size
- Specific surface area
- Void volume
- Partile porosity
- Bark density

Particle size cannot be exactly determined but by screening the particles two times with a well-defined matrix, an upper and lower limit of the particle size can be estimated. The particles are not perfect spheres but sphericity can be calculated. Particle sphericity is a dimensionless number that describes of how high degree a particle is expected to behave as a perfect sphere. The sphericity can according to W. L. McCabe be calculated with Equation 2.5. [7] Where d_p is the particle diameter, s_p the surface area and V_p the particle volume.

$$\Phi_s = \frac{6/d_p}{s_p/V_p} \tag{2.5}$$

The hydraulic diameter, d_h, for a volume can be calculated by first calculating the volume of the object, V_p. When the volume is known the diameter corresponding to a sphere with the same volume can be calculated with Equation 2.6.

$$d_h = 2\left(\frac{3V_p}{4\pi}\right)^{\frac{1}{3}} \tag{2.6}$$

Specific surface area (m^2/m^3) of the bulk in a packed bed needs to be known because the mass transferring area will be a limiting factor. In order to determine the specific surface area the shape of the particles must be known. After the screening of the particles it was noted that the particle shape depends on the particles size, small particles had almost a spherical shape while larger particles tended to be more varied in shape.

Void volume is the volume in the dryer unoccupied by bark where the dying air will flow. In order to determine the actual flow velocity of the air the void volume needs to be known. The actual airflow velocity, v, can be calculated with the Equation 2.7 where G is the inflow of air, r the radius in axial direction of the dryer and ε_b the void space in the bed.

$$v = \frac{G}{\pi r^2 \varepsilon_b} \tag{2.7}$$

The void volume can be estimated by measuring the bark weight and the total volume. The bulk density can be calculated from total weight and volume. Particle density can be approximated with cellulose and the density of air can be found in various table works. When all densities are known Equation 2.8 can be set up, where bulk porosity becomes the only unkown. [8]

$$\rho_b = \rho_p(1 - \varepsilon_b) + \rho_a\varepsilon_b \tag{2.8}$$

What also needs to be considered is that the particle porosity, ε_p, will change over time as the moisture content in the particle will do so. Equation 2.9 takes this phenomena into account, where ρ_b is bed density, ρ_p solid particle density, ρ_l the density for water and u the moisture content. [9]

$$\varepsilon_p = 1 - \frac{\rho_b(1-u)}{\rho_p} - \frac{\rho_b u}{\rho_l} \tag{2.9}$$

Densities of bark have been measured by P. Lehtikangas. It was discovered that the density vary significantly according to the type of tree it comes from. Bark from spruce has a wet density varying from 300-425 kg/m^3 while pine has lower density 275-325 kg/m^3. [10]

The density for the solid phase, ρ_p, is needed for the calculations. Being hard to measure this density it can be estimated to be the density of cellulose which is 1500 kg/m^3.[9]

2.5 Shrinking

Over time as the drying takes place the water content of the particle will get lower, which will result in shrinking. This will result the porosity change as shown in Equation 2.10. [8]

$$\varepsilon_b = 1 - \frac{\rho_b}{\rho_p} \cdot \frac{1 + \frac{\rho_p}{\rho_l}u}{1+u} \tag{2.10}$$

P. Suvarnakuta [4] has suggested a different, empirical, relationship between shrinking and moisture content. The aim for this model is to describe the change in volume instead of change in porosity. This empirical model was done by fitting the relationship to experimental data from drying carrot cubes. a, b and c are empirical constants chosen to best fit the experimental curve. The relationship can be seen in Equation 2.11.

$$\frac{V}{V_0} = a\left(\frac{u}{u_i}\right)^2 + b\left(\frac{u}{u_i}\right) + c \tag{2.11}$$

V_0 is the initial volume and V the volume after drying. u is the total moisture content and u_i is the total initial moisture content. [4]

2.6 Mass and heat transfer coefficients

Due to complex measurements that have to be made to estimate the sphericity and the surface area for bark, a simplification can be made. Instead of having the surface area included in the heat transfer coefficient and thus have a volumetric instead of a surface heat transfer coefficient.

The volumetric mass transfer coefficient can then be estimated from the volumetric heat transfer coefficient by using Reynold's Analogy as can be seen in Equation 2.12.[11]

$$\sigma_a = \frac{ha}{Cp_a + X_a Cp_v} \tag{2.12}$$

2.7 Hygroscopic material

A hygroscopic material is recognized by that the vapor pressure is lower than the vapor pressure of pure water at the same temperature. This happens when water interacts with the bark chips on a chemical level and form chemical bonds. The total energy needed to vaporize the water, ΔH_{vap}, will consist of two parts shown in Equation 2.13, ΔH_0 which is the normal vaporization energy for water, plus ΔH_{sorp} which is the energy needed to break the bonds between water and the bark. [11]

$$\Delta H_{vap} = \Delta H_0 + \Delta H_{sorp} \tag{2.13}$$

It has been observed that the hygroscopic behavior tend to take the shape of a 2nd degree polynomial with up to 1000 kJ/kg bonding energy where the bonding energy is the highest at low moisture content. [12]

Holmberg et al. [9] have done experiments that shows that during low moisture content in bark the partial pressure will start to depart from the partial pressure over pure water. The partial pressure will become lower and therefore limit the mass transfer.

3 Method

The model was written with MATLAB and compared with experimental data from the pilot plant.

3.1 Discretization

In the model the dryer was split into several stages, as can be seen in Figure 3.1, with the temperature, $Ta_{in,}$ and air moisture content, $Xa_{in,}$ entering one element being the temperature, $T_{a,}$ and moisture content, $X_{a,}$ leaving the one before. The dryer was split into n elements, making the height, h, of each cell the total length of the dryer divided by the number of stages, n.

Between each stage prefect mixing is assumed. So the air that have been in contact with smaller particles with higher specific area, which leads to higher heat and mass transfer, will have the same moisture content and temperature when entering the next cell as the air that was in contact with the larger particles.

With n levels in the dryer the temperature and air saturation for each level can be calculated and compared with experimental data corresponding to the same level.

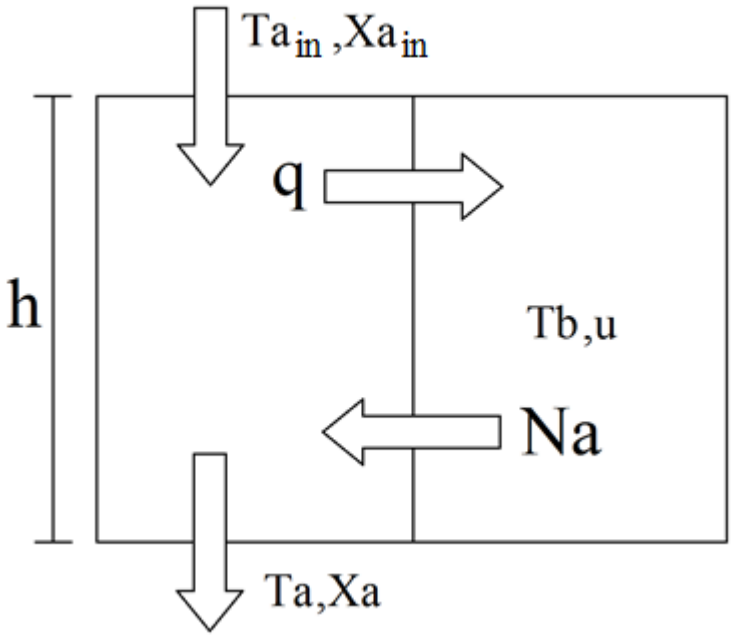

Figure 3.1. Mass and heat balance visualization

3.2 Heat and mass transfer equations

The model was written as semi-empirical with temperature and saturation differences as driving force with ha and σa as volumetric heat and mass transfer coefficients.

The heat and mass transfer coefficients was written as volumetric simply because it was difficult to estimate the actual surface area or bark. The reasons for this are because the size distribution was wide and geometry varied a lot. The heat flux, q, over each element with volume V_e, calculated with Equation 3.1 was set up as in Equation 3.2 with temperature difference as the driving force. The mass flux, Na, was set up over the same volume with difference in saturation as driving force as in Equation 3.3.

$$V_e = \pi r^2 h \tag{3.1}$$

$$q = (T_a - T_b) h a V_e \tag{3.2}$$

$$Na = (X_n - X_a) k g a V_e \tag{3.3}$$

3.3 Isotherm

Holmberg at al. [9] experiments show results that indicate that at lower moisture content the water pressure above the bark will deviate from the pressure of pure water at same temperature. In order to calculate the actual water pressure above the bark both temperature and moisture content in the bark needs to be taken into account.

The pure water pressure as a function of temperature was estimated by using Antoine's equations [11] with the following constants:

$a = 8.07131, b = 1730.63$ & $c = 233.426$

This gives absolute pressure in mmHg from temperatures in °C, which was recalculated to bar by dividing with 750.06 mmHg/bar as can be seen in Equation 3.4.

$$P_{sat} = \frac{10^{a - \frac{b}{c + T_b}}}{750.06} \tag{3.4}$$

Guggenheim Anderson De Boer (GAB) method was used to fit the experimental data at low moisture content.

Equation 3.5 shows the general form for the GAB equation, where parameters V_m, c and k are material-specific properties while φ is the partial pressure of water in air and u the moisture content in the bark.

$$u = \frac{Vmck\varphi}{(1 - k\varphi)(1 + (c - 1)k\varphi)} \tag{3.5}$$

During the literature review no constant for the bark were found but various wood properties were found. Mean values for the constants were calculated by combining values for different wood types. These values are:

$$V_m = 0.08, c = 9 \ \& \ k = 0.65$$

Then parametric sweeps were performed by varying all three variables plus/minus 20 % and validate the resulting plot against the data points from the experiments. The strength of the correlation was weighted with the coefficient of determination, R^2, method. Where the constants below gave the best fit for spruce, resulting in $R^2 = 0.986$.

$V_m = 0.0832, c = 10.80 \ \& \ k = 0.6760$

This result can be seen in Figure 3.2.

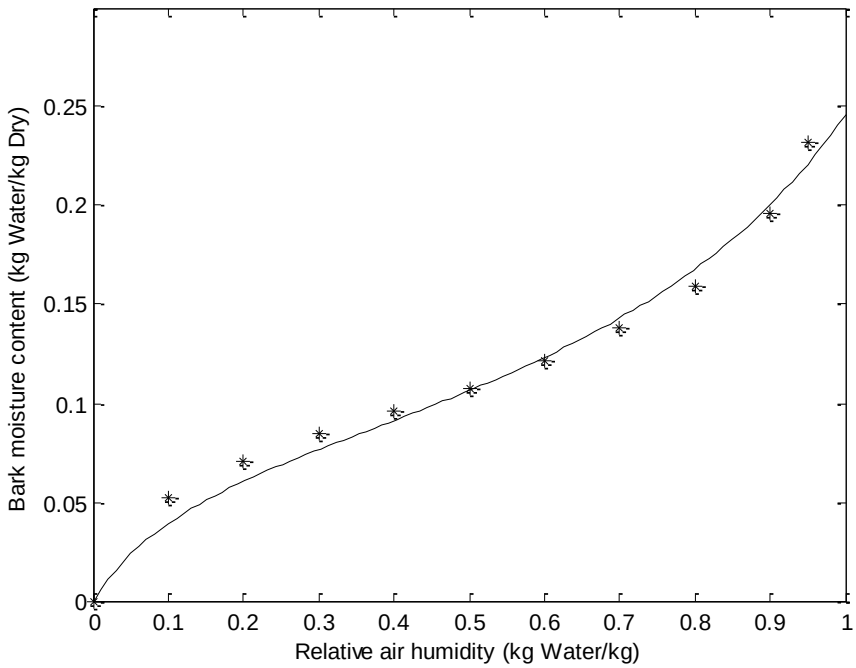

Figure 3.2. Bark moisture content as a function of air humidity

When modeling the partial pressure of water as a function of moisture content is of interest so the GAB equation was rewritten accordingd to Equation 3.6.

$$u = \frac{Vmck\varphi}{(1-k\varphi)(1+(c-1)k\varphi)}$$

$$u(1 + ck\varphi - k\varphi - k\varphi - ck^2\varphi^2 + k^2\varphi^2) = Vmck\varphi$$

$$\varphi(uck - 2uk - Vmck) = \varphi^2(vck^2 - vk^2) - u$$

$$k_1 = (uck - 2uk - Vmck)$$
$$k_2 = (vck^2 - vk^2)$$
$$k_3 = u$$

$$\varphi = \frac{\sqrt{k_1^2 + 4k_2k_3} + k_1}{2k_2} \tag{3.6}$$

By multiplying the relative humidity with the vapor pressure of pure water the function for vapor pressure at low moisture content was obtained, as can be seen in Equation 3.7.

$$P_{iso}(u, T_b) = \varphi(u)P_{sat}(T_b) \tag{3.7}$$

By plotting Equation 3.7 over an interval of moisture content in the bark at constant temperature together with the vapor pressure of water at the same temperature, it can be seen that the pressure for the isotherm will increase above the pressure for pure water at higher moisture content. It was found graphically that the function for the isotherm will surpass the value of the absolute pressure at u = 0.245 kg water/kg dry bark.

In order to get a good representation of the vapor pressure above the bark a conditions was introduced which will take the value from the isotherm, Equation 3.7, if u is below 0.245 and pressure for pure water, Equation 3.4, if above. The graphic interpretation of this is the solid lines in Figure 3.3.

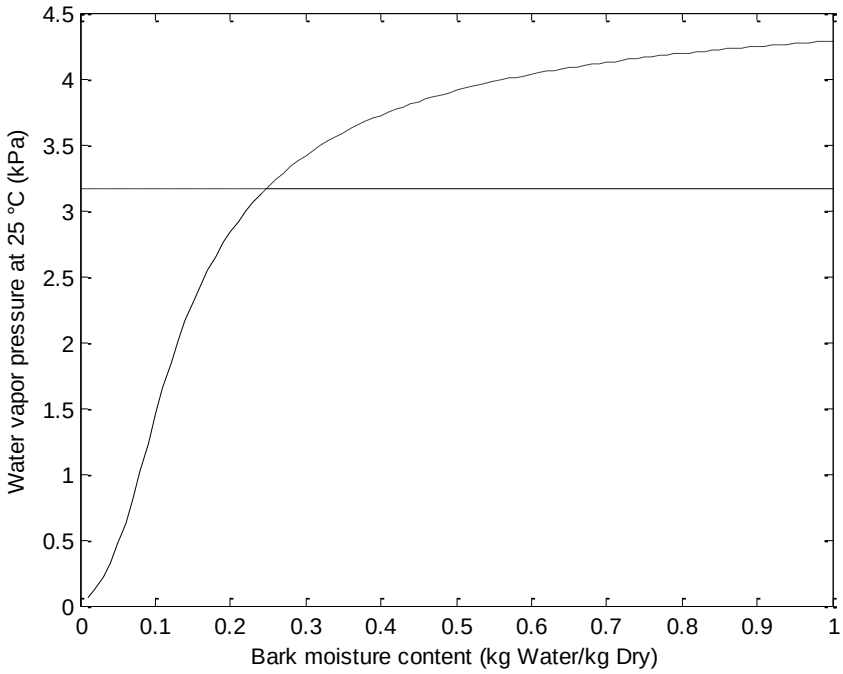

Figure 3.3. Air humidity as a function of bark moisture content

3.4 Heat of sorption

The heat of sorption behavior was modeled like a 2nd degree polynomial with heat of sorption energy of 1000 kJ/kg at u=0. The heat of sorption was modeled to take effect at the same time as the isotherm, at u=0.245kg water/kg dry bark. Equation 3.8 was used to increase the total energy needed to vaporize the water from 2500 kJ/kg at u=0.245 to 3500kJ/kg at u=0.

$$\Delta H_{vap} = 3500 - 1.666 \cdot 10^4 u^2 \quad (3.8)$$

3.5 Model

Initially the model was done with one heat transfer and one corresponding mass transfer coefficient for the whole bark bed. Due to that simplicity the drying rate for this model did not correspond with the experimental data during all drying phases.

Instead a model with three size fractions was used. This was done by screening of the bark two times, at 10 & 2 mm and thus generating three fractions: Below 2 mm, 2-10 mm and above 10 mm.

The weight for each fraction was measured and weight fractions were calculated. When the fractions sizes were known two set of variables were introduced, a heat transfer coefficient for each fraction, h_a, and the size of the fraction, F. Also the bark temperature, T_b, was split up into three separate variables since the smaller particles have a higher specific surface area and will therefore have a higher heat transfer coefficient which will lead to that they will heat up faster.

The heat flux into the particles, q_n, will then be modeled as Equation 3.9, where ha_n is the heat transfer coefficient for particles and F_n the mass fraction for particle size n, n=1,2,3.

$$q_n = (T_a - T_{bn}) ha_n V_e F_n \tag{3.9}$$

The total heat transfer from the air to the bed therefore becomes the sum of each separate heat flux, according to Equation 3.10.

$$q_t = \sum_{n=1}^{3} q_n \tag{3.10}$$

In the same way the mass flux will be split into three parts with three mass transfer coefficients and the same fractions sizes, where the mass transfer coefficients are calculated with Reynold's analogy as in Equation 3.11.

$$\sigma a_n = \frac{ha_n}{Cp_a + X_a Cp_v} \tag{3.11}$$

In order to calculate the mass flux from the bed to the air, X_n at the surface of the bark in the air needs to be known. X_n is calculated by using either Equation 3.12 when above the isotherm of Equation 3.13 when below.

$$X_n = \frac{0.62 P_{sat}(T_{bn})}{1.01325 - P_{sat}(T_{bn})} \tag{3.12}$$

$$X_n = \frac{0.62 P_{iso}(u_n, T_{b_n})}{1.01325 - P_{iso}(u_n, T_{b_n})} \tag{3.13}$$

When X_n is known the mass flux can be set up according to Equation 3.14.

$$Na_n = (X_n - X_a)\sigma a_n V_e F_n \tag{3.14}$$

The total flux of water from the bed to the air will be the sum of all mass fluxes, according to Equation 3.15.

$$Na_t = \sum_{n=1}^{3} Na_n \tag{3.15}$$

With the total flux known together with the air flow rate the difference in X_a can be calculated by dividing the mass flux with $G\Delta t$, which is the total air mass for each iteration as in Equation 3.16.

$$\frac{dX_a}{dt} = Na_t \frac{1}{G\Delta t} \tag{3.16}$$

The drying rate for the bark can then be set up as the reverse water flux divided by the mass of bark in each cell as in Equation 3.17.

$$\frac{du_n}{dt} = -\frac{Na_n}{V_e \rho_b F_n} \tag{3.17}$$

The temperature change of the bark can be derived by looking at the heat flux going into and leaving the bark. The heat flux going into the bark is q_n. The heat flux leaving the bark is the difference between the states of the water in the bed and water vapor at temperature T_b multiplied by the water flux. The difference in heat fluxes in then divided by the heat capacity of the bed at moisture content u_n and temperature T_b as can be seen in Equation 3.18.

$$\frac{dT_{b_n}}{dt} = \frac{q_n - Na_n\left((Cp_v - Cp_l)T_{b_n} + \Delta H_{vap}\right)}{\left(Cp_b(T_{b_n}) + Cp_l u_n\right)\rho_b V_e F_n} \tag{3.18}$$

Unlike the bark bed the air was not divided into separate fractions. In order to set up the temperature derivative for the air the average bark temperature was calculated with Equation 3.19.

$$T_b = \sum T_{bn} F_n \tag{3.19}$$

With the average temperature calculated for the bark bed the temperature derivative for the air can be set up like Equation 3.20 below. Where the heat flux, q_t,is the sum of q_n which the energy required to heat the vapor from bark temperature to air temperature is added and divided by the heat capacity of air with moisture content X_a.

$$\frac{dT_a}{dt} = \frac{-q_t + Na_{tot} Cp_v (T_b - T_a)}{G\Delta t (Cp_a + X_a Cp_v)} \tag{3.20}$$

3.6 Initial and inlet values

For initial values for the bark and inlet conditions for the air both measurements and assumptions have been made.

Inlet air temperature has been varied between 50 and 130 °C with a 20 °C interval in the experiments and same values have been used in simulations.

The inlet moisture content for the air, X_0, has been assumed to be 70 % relative humidity at 5 °C, which was the outdoor conditions for the majority of the experiments.

Initial temperature for the bark bed was set to room temperature, 20 °C.

Initial moisture content, u, was calculated from the sampled weight data according to Equation 3.21 where m is the total bark mass.

$$u0 = \frac{m_0}{m_{end}} - 1 \tag{3.21}$$

Dry bulk density was calculated by dividing with the weight by volume of the dryer at the start and the end as in Equation 3.22.

$$\rho_b = \frac{m_{end}}{V} \tag{3.22}$$

Dry air flow rate was calculated by measuring mass flow in an orifice plate and recalculate to velocity with geometrical correlations and air density. For these experiments an air velocity of 0.4 m/s was used in a pipe with radius of 0.15 m which gives a dry air flow, G, with assumed air density 1 kg/m^3, of 0.0284 kg/s according to Equation 3.23.

$$G = \frac{\pi r^2 v_o \rho_a}{1 - X_0} \tag{3.23}$$

3.7 Model variations

In total four model variations will be presented, the models and their specifications are listed below.

3.7.1 Adiabatic saturation model

In this model it is assumed that the air entering the dryer will get saturated before leaving. This was carried out by setting the heat and mass transfer coefficient to a high value.

3.7.2 Heat and mass transfer coefficients

In this model the heat and mass transfer coefficients have been varied to get the best representation of the drying curve.

3.7.3 Isotherm model

In this model the heat and mass transfer coefficients from the heat and mass transfer model have been used but also the effect of the isotherm have been added. The isotherm will decrease the drying rate at low moisture content.

3.7.4 Fraction model

For this model the bark were screened into three size fractions. The size of each fraction was measured and assigned an individual heat transfer coefficient. The effect of the isotherm was still added together with increasing heat of vaporization. Each heat transfer coefficient was varied in order to get the best representation of the drying curve.

3.8 Experimental setup

Hot air in the temperature range of 50°C – 130°C will enter in the top of the dryer. The initial temperature for the bark bed is room temperature, set to 20°C. Ingoing air velocity is measured and during the experiment the total weight and the temperature at each thermocouple is measured until the bark bed is totally dry. In Figure 3.4 a sketch of the experimental setup can be seen. The dryer dimensions are radius 0.15 m and bed height 0.63 m.

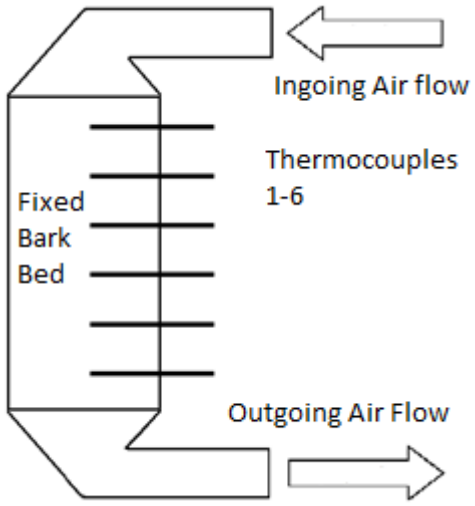

Figure 3.4. Sketch of the dryer setup

3.9 Fitting to experimental data

The model was fitted to experimental data by comparing the weight and temperature profiles from the model with the experiments. The coefficient of determination, R^2, was used to indicate the degree of fitting between the models weight curve and the data.

The coefficients that were varied when fitting to data were the heat transfer coefficients, ha, which indirectly through Reynold's analogy also varies the mass transfer coefficients, σa.

The heat transfer coefficients were varied between 0.5 kW/m^3°C - 2.5 kW/m^3°C together with the condition that the heat transfer coefficient must be larger for smaller particles and vice versa.

The optimization of the heat transfer coefficients was done at 90°C inlet air temperature and then extrapolated down to 50°C and up to 130°C.

3.10 Solver

The mass and energy balances were solved with Matlab by using an ODE solver. The ODE solver was run for the same time as the experiments in order to get a good comparison between the model and the experimental data. The optimization of the coefficient of determination was done with a for-loop for each heat transfer coefficient and the coefficient of determination was calculated for each set of heat transfer coefficients.

3.11 Losses

Mass losses include volatile non-water components that may leave with the air outlet. In order to minimize mass losses in the pilot setup a piece of cloth have been placed covering the outlet. Estimation of mass losses will be very difficult because no measurements have been done. But mass losses are most probably neglect able as the amount that will be able to leave the system through the cloth in the bottom will be very small compared to the total mass.

Heat losses were measured by running air through already dry bark and measure the temperature in the bottom and top. After equilibrium had set in, the thermocouples were swapped to eliminate eventual calibration errors. There were no consistent heat losses measured and therefore heat losses was neglected in the model.

3.12 Economic aspect

The interesting aspect of drying is that one can use low value heat to increase the amount of high value heat. Low pressure steam can be used to dry bark, the low value heat in will be regained as high value heat in the bark as it will both increase the combustion temperature and the heating value of the bark.

Also by splitting up the drying in several stages would decrease the quality needed of the low pressure steam, but the total heat demand will be the same. [6]

3.13 Measurement errors

As mentioned above the temperature measurements have been done with eight sensors evenly distributed along the dryer. By looking at the temperature profiles it can be seen that there is some unexpected behavior. At some points the temperature is shown to be higher further down in the dryer. The reasons for this deviation could be caused be inaccuracies in the measurements or caused by locally uneven distribution of the bark which would disturb the temperature profile.

The moisture content have not directly been measured instead the total weight of the dryer have been measured. By looking at the results fluctuations can be seen.

4 Results and Discussion

In these results data from experiments and the different models will be presented where the improving results are notable, starting with the simplest model and moving on to the final.

4.1 Results from experiments

For all experiments initial moisture content, kg water/kg dry matter, was calculated. In Table 4.1 the desnitiy corresponding to different bark types and inlet temperatures can be seen. It is clear that the initial moisture content vary a lot between different bark types.

Table 4.1. Initial moisture content for the experiments, kg water/kg dry matter

Bark Type	**50 °C**	**70 °C**	**90 °C**	**110 °C**	**130 °C**
Birch	0.35	0.50	0.58	0.66	0.65
Spruce	1.39	1.27	1.39	1.57	1.46
Pine	1.69	2.00	2.07	1.98	1.96

- *Birch 0.35-0.65 kg Water/kg dry matter*
- *Spruce 1.27-1.57 kg Water/kg dry matter*
- *Pine 1.69-2.07 kg Water/kg dry matter*

The dry densities were also calculated and also here clear differences between bark types are observed. In Table 4.2 dry bulk densities can be seen.

Table 4.2. Dry bulk density for the experiments, kg dry matter/m^3

Bark Type	**50 °C**	**70 °C**	**90 °C**	**110 °C**	**130 °C**
Birch	286	260	248	241	227
Spruce	132	136	125	129	136
Pine	146	140	133	134	129

- *Birch 227-286 kg/m^3Dry*
- *Spruce 125-136 kg/m^3 Dry*
- *Pine 129-146 kg/m^3 Dry*

4.2 Adiabatic saturation

It was assumed that the air will reach saturation before leaving the dryer. In order to test if this was true a model with a high heat transfer coefficient was set up, leading to that the air almost instantly becomes saturated as soon as it enters the bed. In Figure 4.1.a the weight curve for spruce can be seen, one dashed line that represents the weight curve for the experiment with spruce at 90°C and the model in solid with one high heat transfer coefficient, ha=10 kW/m^3°C. It can be seen in all figures that the drying rate for all bark types will be too high; especially at low moisture content were the internal transport is the limiting factor. It can be seen in Figure 4.1.b that the drying rate in the linear phase is too high for birch. This is due to the lower initial moisture content which will lead to that internal transport will limit the drying earlier. Figure 4.1.c shows the weight curve for pine which looks similar to spruce, which is expected as the initial moisture content is more similar to spruce than birch.

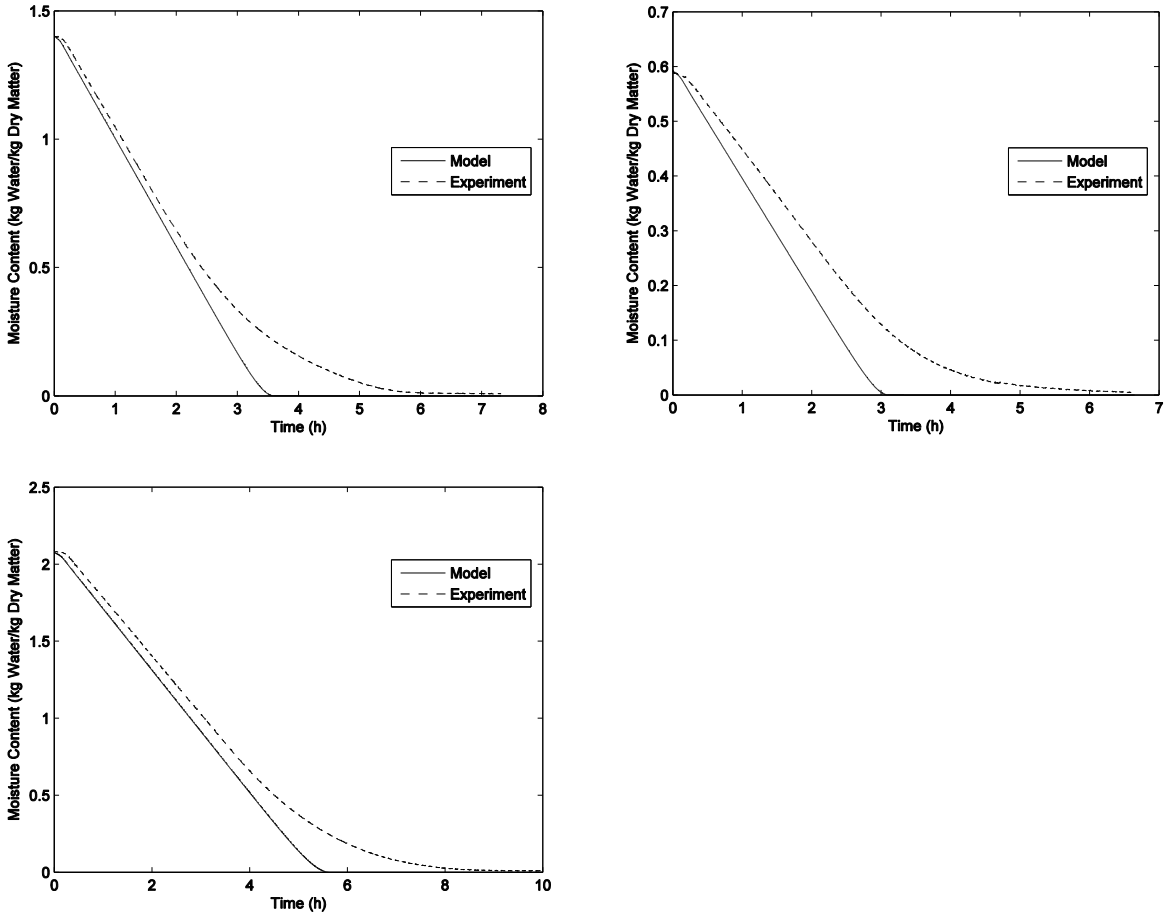

Figure 4.1.a Spruce weight curve for saturated assumption at 90 °C. Figure 4.1.b Birch weight curve for saturated assumption at 90 °C. Figure 4.1.c Pine weight curve for saturated assumption at 90 °C

In Figure 4.2.a the temperature profiles for the bark can be seen. The high heat transfer coefficient causes the bed too instantly go from adiabatic saturation temperature to air temperature as soon as it is dry. Even though the temperature profiles do not have the characteristic shape as the experimental data, it still gives a good representation on where the drying occurs in the bark bed as the heating up from adiabatic saturation temperature starts at approximately the same time.

In Figure 4.2.b the air saturation profiles show that the outgoing air will almost be saturated for the entire simulation, which was achieved by increasing the heat transfer coefficient.

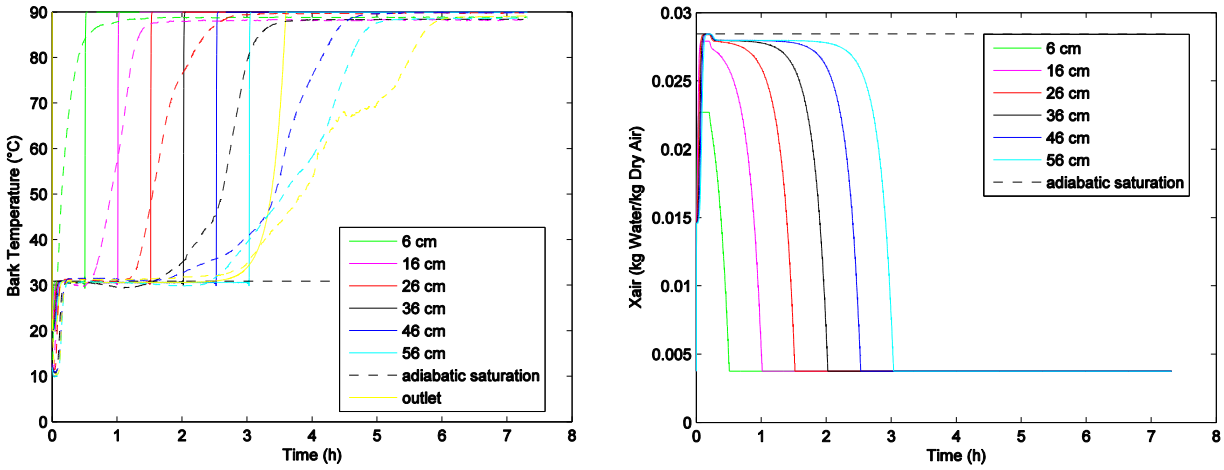

Figure 4.2.a Spruce temperature profiles for saturated assumption at 90 °C. Figure 4.2.b Spruce air saturation profiles for saturated assumption at 90 °C

4.3 Heat transfer and mass transfer coefficients

The same model that was used for the adiabatic saturation assumption was used again, now with lower heat transfer coefficients to match the profile for the drying rate. The heat transfer coefficents that was used was the coefficient for the largest particle size in the fraction mode. In this way much better representations for the drying curves were achieved. In Figure 4.3 the result can be seen, it is clear that both birch (b) and pine (c) fits well to this model but the linear phase for spruce (a) does not match the experimental data as well.

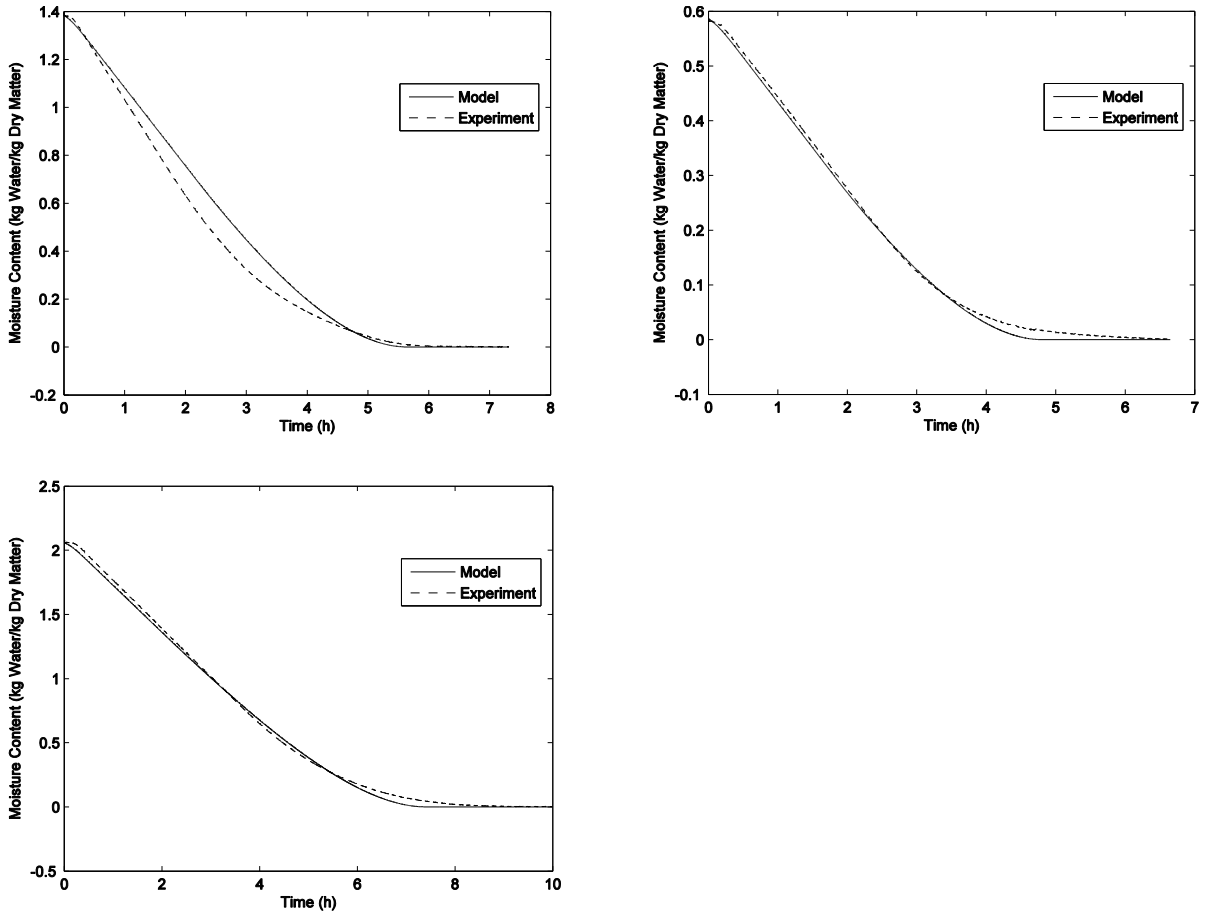

Figure 4.3.a Spruce weight curve for heat transfer coefficient, ha=0.9 kW/m^3°C, at 90 °C
Figure 4.3.b Birch weight curve for heat transfer coefficient, ha=0.9 kW/m^3°C, at 90 °C
Figure 4.3.c Pine weight curve for heat transfer coefficient, ha=1.5 kW/m^3°C, at 90 °C

In Figure 4.4.a it can be seen that the temperature profiles now get a slightly smoother shape at the higher temperatures and the entire profile is shifted to the right. This is due to the lower heat transfer coefficient which causes each element to heat slower.

In Figure 4.4.b it can now be seen that the air will not reach saturation before leaving the bed. The air will instead reach the maximum possible saturation for current heat transfer coefficient and bed height and level out at that value until the bed starts to dry in the top of the dryer. When the top becomes dry the total mass transfer over the entire dryer will start to decrease which naturally leads to that saturation in outgoing air will decrease.

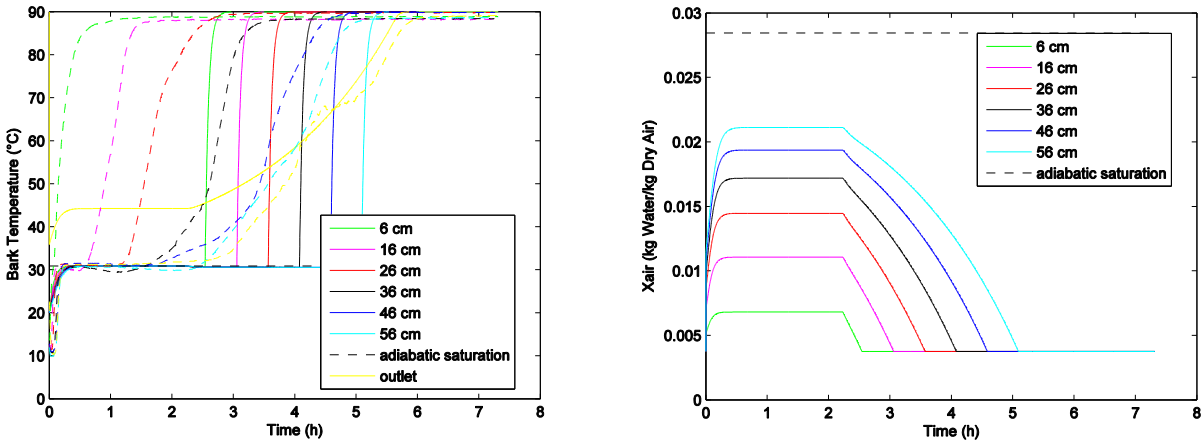

Figure 4.4.a Spruce temperature profiles for heat transfer coefficient, ha=0.9 kW/m^3 °C, at 90 °C. Figure 4.4.b Spruce air saturation profiles for heat transfer coefficient, ha=0.9 kW/m^3°C, at 90 °C

4.4 Isotherm model

For this model the effect of the isotherm was added. In Figure 4.5 it can be seen that the total drying rate was not affected very much by this. This is due to the fact that the isotherm will only take effect at moisture content below 0.245kg water/kg dry matter. For spruce and pine the difference between the drying rates are hardly noticeable but for birch, which have initial moisture content of 0.58 kg water/kg dry matter, the difference is more clear.

The isotherm model gives a good representation of the drying curve for pine and birch but for spruce the model still does not give a good fit. It can be seen in Figure 4.5.a with a low heat transfer, ha=0.9, and Figure 4.6 with a higher heat transfer, ha=1.5, that low ha values give a too slow linear drying phase and a higher drying rate will give a good linear drying rate but gives a bad representation when approaching dry matter.

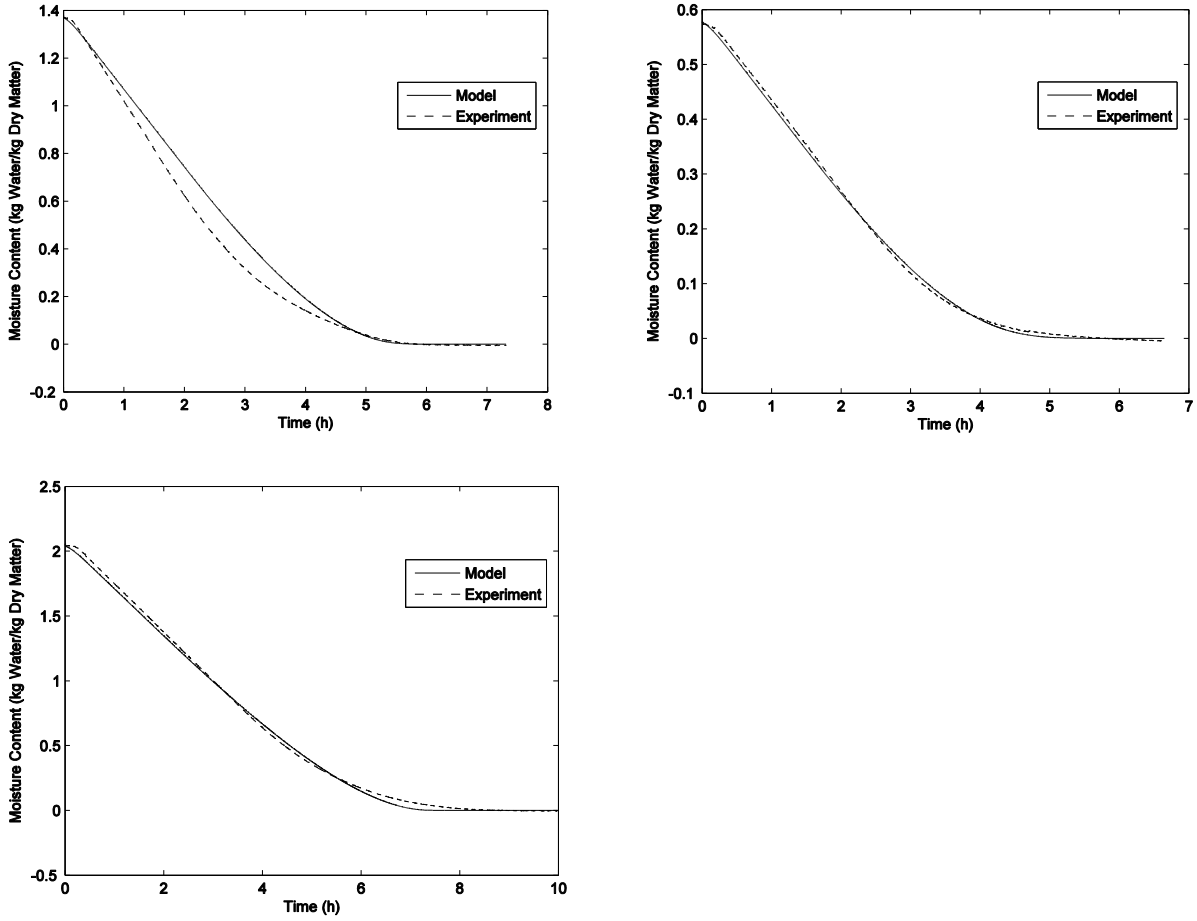

Figure 4.5.a Spruce weight curve for isotherm model, ha=0.9 kW/m^3°C, at 90 °C. Figure 4.5.b Birch weight curve for isotherm model, ha=0.9 kW/m^3°C, at 90 °C. Figure 4.5.c Pine weight curve for isotherm model, ha=1.5 kW/m^3°C, at 90 °C

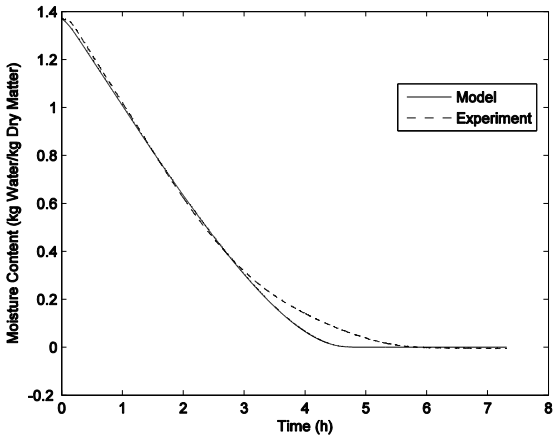

Figure 4.6 Spruce weight curve for isotherm model, ha=1.5kW/m^3°C, at 90°C

In Figure 4.7 is can be seen that he temperature profiles now takes the shape of the experimental data even more as the drying rate will be lowered by the isotherm at the end of the process, which is where the temperature starts to increase. Leading to that the temperature profiles will get the more S-shaped profiles. However there is still an offset between the experimental data and the models temperature profiles, especially for spruce and pine which has higher initial moisture content.

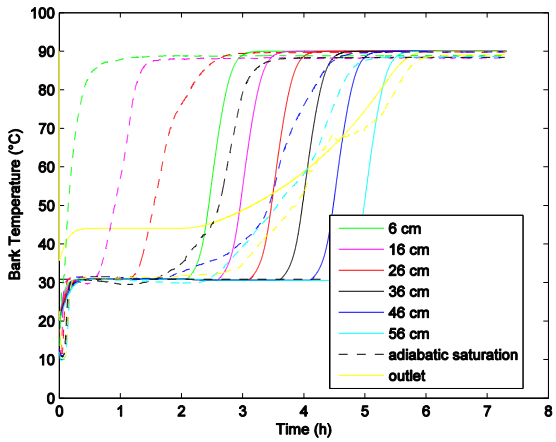

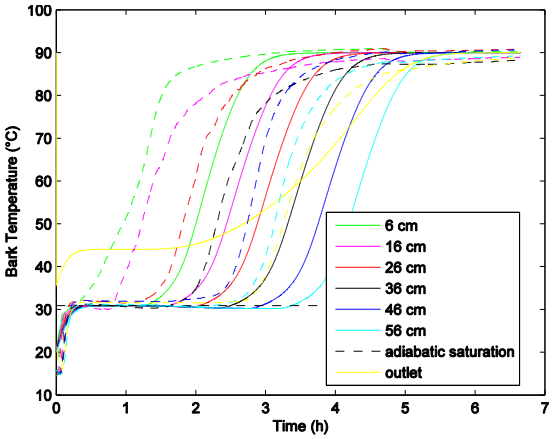

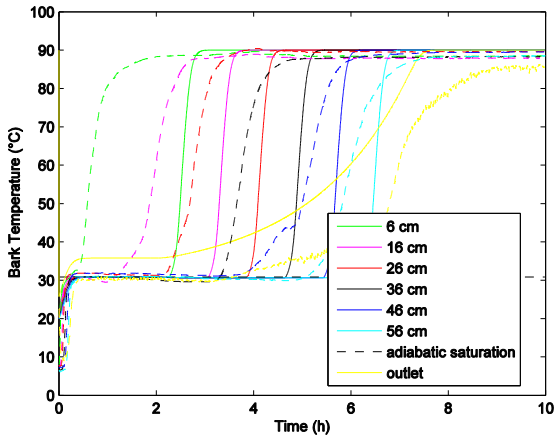

Figure 4.7.a Spruce temperature profiles for isotherm model, ha=0.9 kW/m^3°C, at 90 °C.
Figure 4.7.b Birch temperature profiles for isotherm model, ha=0.9 kW/m^3°C, at 90 °C.
Figure 4.7.c Pine temperature profiles for isotherm model, ha=1.5 kW/m^3°C, at 90 °C

Figure 4.8 shows that the air saturation profiles also get a bit more smoothened due to the isotherm as it will take longer for moisture to enter the air when approaching dry matter. Also the air still does not get saturated before leaving the bark bed.

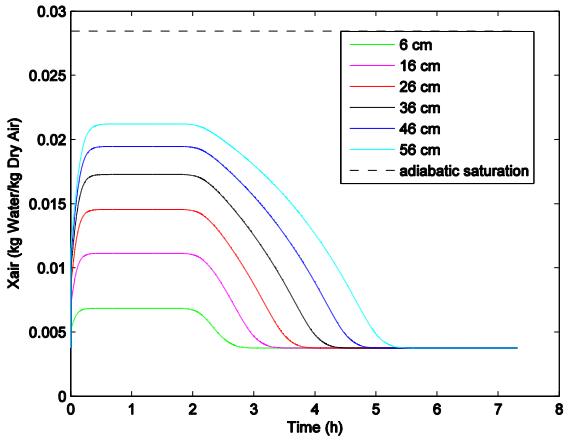

Figure 4.8. Spruce air saturation profiles for isotherm model, ha=0.9 kW/m^3°C, at 90 °C

In Figure 4.9.a-4.9.d the drying rate for spruce at temperatures 50, 70, 110 and 130 °C can be seen. It is clear that there is a consistent offset between the experimental spruce drying rate and the drying rate calculated from the model. This both shows that the deviation between the experiment and model at 90 °C most likely is not caused by an experimental error and that a better model is needed to get a good representation of the drying rate of spruce, the model of choice was a fraction model.

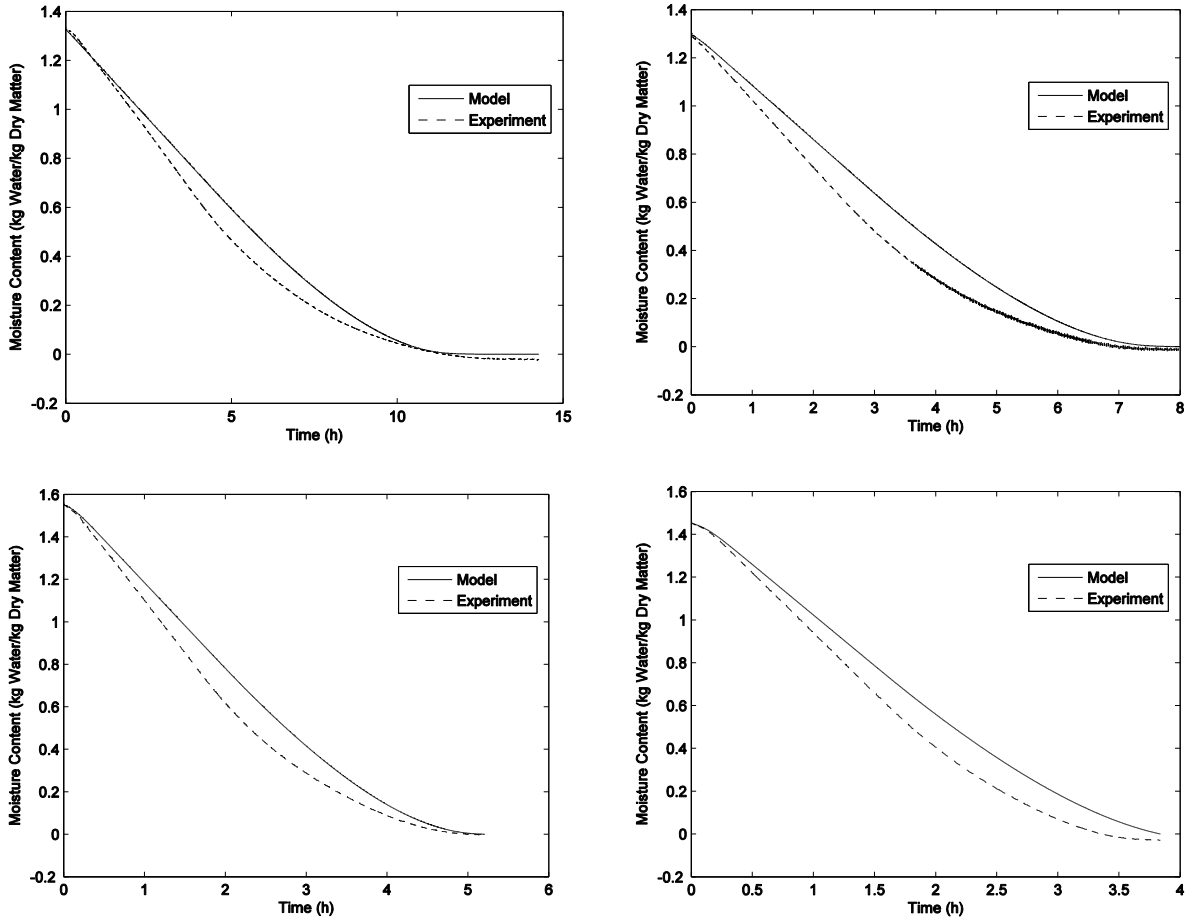

Figure 4.9.a Spruce weight curve for isotherm model, ha=0.9 kW/m^3°C, at 50 °C
Figure 4.9.b Spruce weight curve for isotherm model, ha=0.9 kW/m^3°C, at 70 °C
Figure 4.9.c Spruce weight curve for isotherm model, ha=0.9 kW/m^3°C, at 110 °C
Figure 4.9.d Spruce weight curve for isotherm model, ha=0.9 kW/m^3°C, at 130 °C

4.5 Fraction model

In Table 4.3 the result for the screening of the bark can be seen. In order to get an even better representation of the drying rate, especially for spruce, a fraction model was made from the data from the screening.

Table 4.3. Mass fraction sizes for bark types

Bark Type	Below 2 mm	2-10 mm	Above 10 mm
Spruce	0.063	0.449	0.488
Birch	0.174	0.435	0.391
Pine	0.018	0.267	0.715

Each fraction was assigned a heat transfer coefficient and was varied between 0.5 kW/m^3°C and 2.5 kW/m^3°C. In Table 4.4 the heat transfer coefficient for each fraction can be seen. The values were obtained by maximizing the coefficient of determination, R^2, against the experimental weight curves at 90°C.

Table 4.4. Heat transfer coefficient corresponding to fraction sizes

Bark Type	Ha1	Ha2	Ha3
Spruce	2.5	1.7	0.9
Birch	1.3	1.1	0.9
Pine	2.5	2.1	1.5

With the heat transfer coefficients in Table 4.4 and fractions sizes in Table 4.3 the model was extrapolated from 90°C down to 50°C and up to 130°C. In Table 4.5 the coefficient of determination, R^2, for these extrapolations can be seen. Note that the R^2 value became very low for birch at 70°C, this mostly likely due to an experimental error as all others got a R^2 above 98.5 %.

Table 4.5. Coefficient of determination for weight curves with fraction model

Bark Type	50 °C	70 °C	90 °C	110 °C	130 °C
Spruce	0.993	0.987	0.996	0.994	0.991
Birch	0.998	0.924	0.999	0.994	0.995
Pine	0.987	0.987	0.996	0.993	0.996

In Figure 4.10.a it can be seen that this model gives a much better representation for spruce, the deviation at the linear phase is almost eliminated and it still gives a good fit at the end of the drying curve. This improvement comes from that the fact that the model will allow differences in heat transfer coefficient between different fractions. In Figure 4.10.b and 4.10.c it can be seen that there is not any major differences for the weight curves for birch and pine. This result is also reflected in Table 4.4 as differences between the heat transfer coefficients for birch and pine are smaller than the ones for spruce.

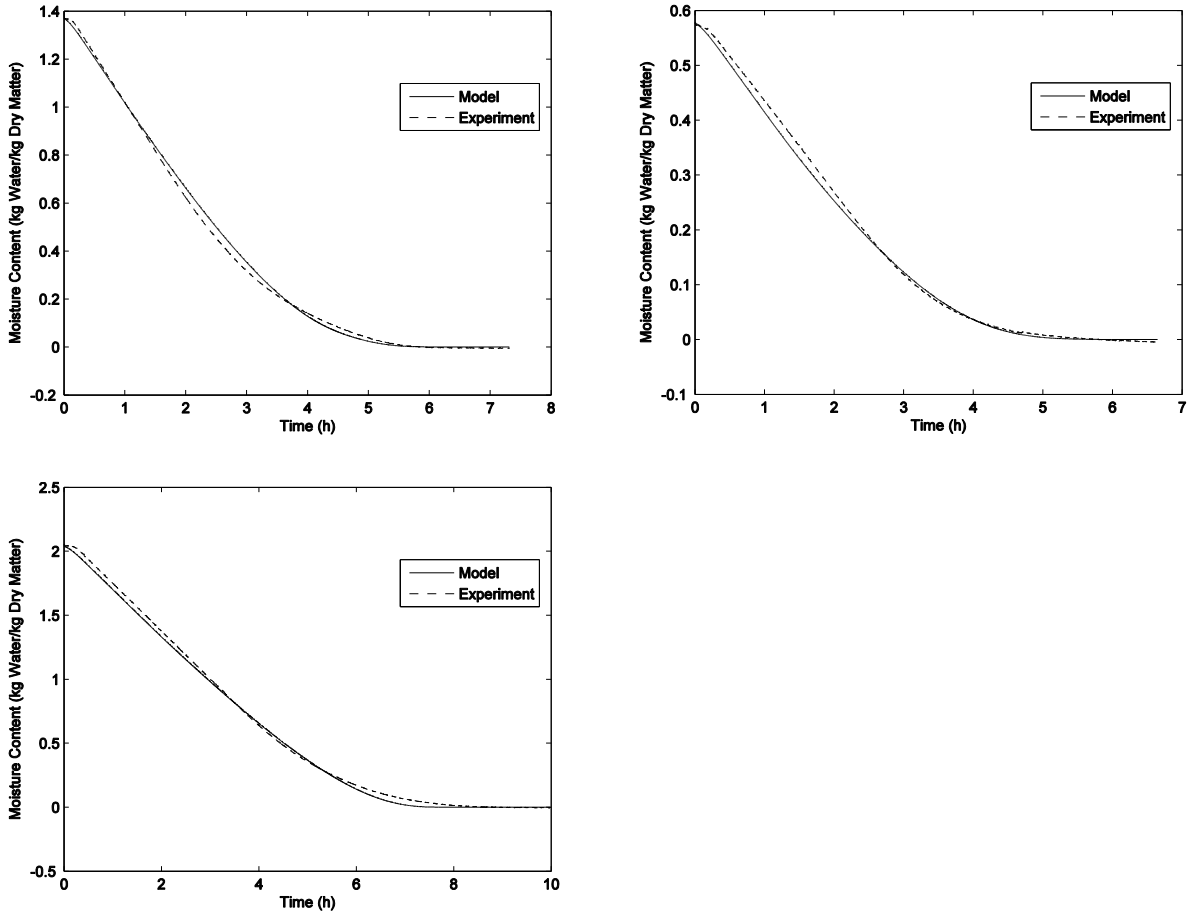

Figure 4.10.a Spruce weight curve for fraction model at 90 °C. Figure 4.10.b Birch weight curve for fraction model at 90 °C. Figure 4.10.c Pine weight curve for fraction model at 90 °C

In Figure 4.11.a the temperature profiles for spruce can be seen, it is very clear that there is a plateau at around 60°C; this is because of the difference of the heat transfer coefficient for the two major particle sizes. It can be seen in Table 4.4 that the optimal heat transfer coefficients for spruce were 1.7 kW/m^3°C for particles between 2 & 10 mm and 0.9 kW/m^3°C for particles above 10mm. In Figure 4.12 it can also be seen that the difference in heat transfer coefficient will affect the air saturation profiles in the same plateau looking way.

In Figure 4.11.b it can be seen that there are not any major difference between the isotherm model and fraction model for birch. The increase in heat of vaporization is clearest for birch; this is due to the lower initial moisture content which causes the average heat of vaporization too increase as a larger part of the total water will be affected by the isotherm. This can be seen in Figure 4.11.b as the temperature profiles will level out slightly below the adiabatic saturation temperature.

For spruce, in Figure 4.11.c there is a small plateau at 45°C, the reason for this is the same as for spruce with the only difference that the plateau will be at a lower temperature as the fraction that gets heated first, the fraction with highest heat transfer coefficient, is smaller than for spruce.

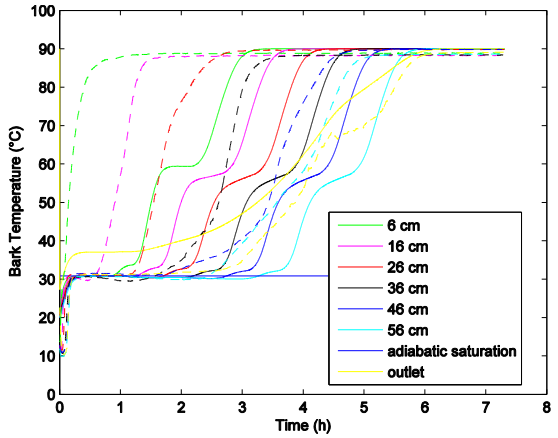

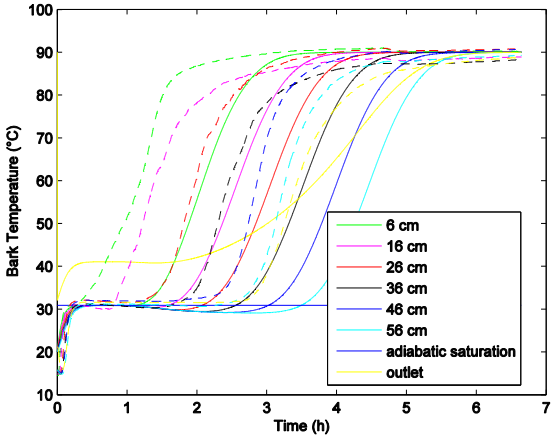

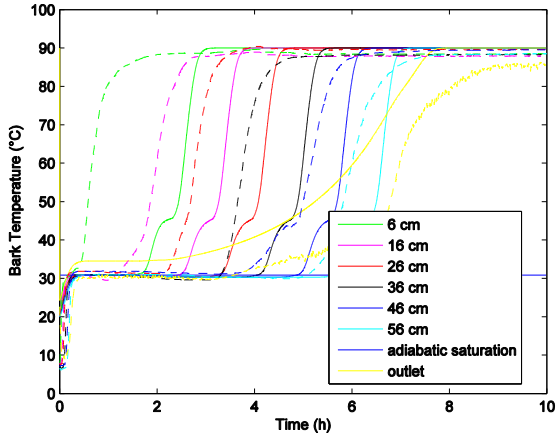

Figure 4.11.a Spruce temperature profiles for fraction model at 90 °C. Figure 4.11.b Birch temperature profiles for fraction model at 90 °C. Figure 4.11.c Pine temperature profiles for fraction model at 90 °C

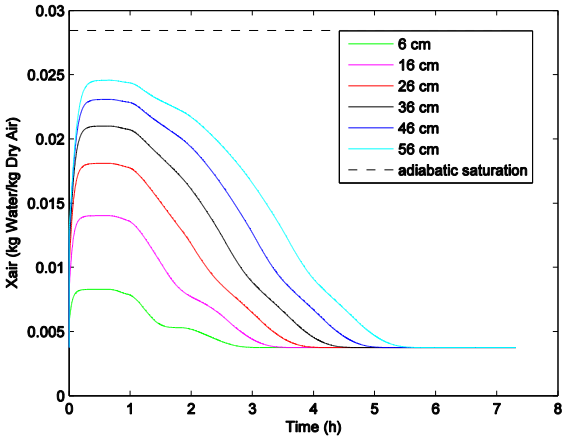

Figure 4.12 Spruce air saturation profiles for fraction model at 90 °C

4.6 Comparison with industrial data

The final fraction model was compared with industrial data from Södra Cell Värö. The density of the bark was set to 130 kg/m^{3}as the majority of the wood from the plant consists of spruce.

The data from the plant consisted of ingoing and outgoing moisture content of the dryer. In total there where 90 data points that had enough information to run the simulation. As the measurements had been done with sampling, there were some unexpected values. In total 12 points was discarded due to unrealistically high or negative drying rates.

The ingoing moisture content and air temperature was obtained from the data and the model was run for the same residence time.

In Figure 4.13 measured moisture content have been plotted against expected moisture content together with the line "measured moisture content = calculated moisture content". It can be seen that the model manages to represent the reality well. Figure 4.14 was also done in order to easier survey the data, calculated moisture content was divided by measured and values was set in intervals. A peak can clearly be seen in the middle of the intervals which suggest that the actually drying rate is well represented.

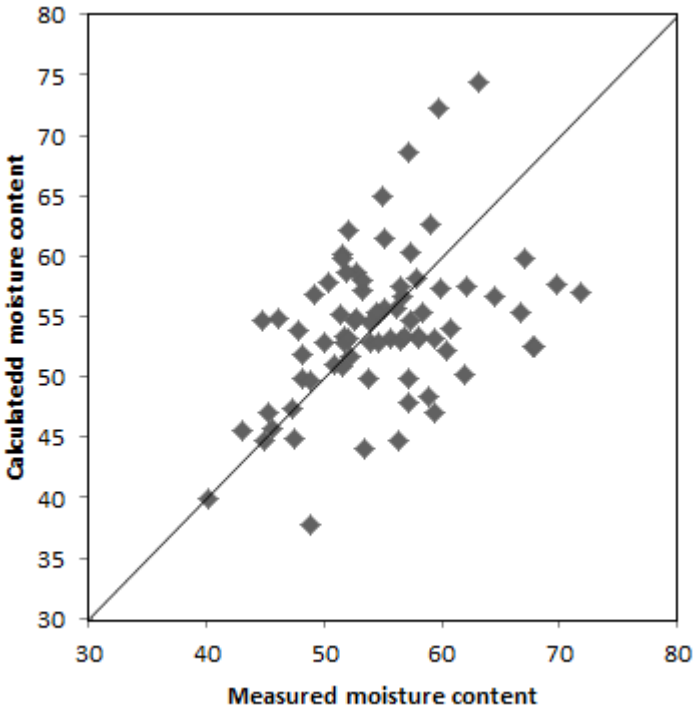

Figure 4.13. Measured moisture content plotted against the models calculated moisture content

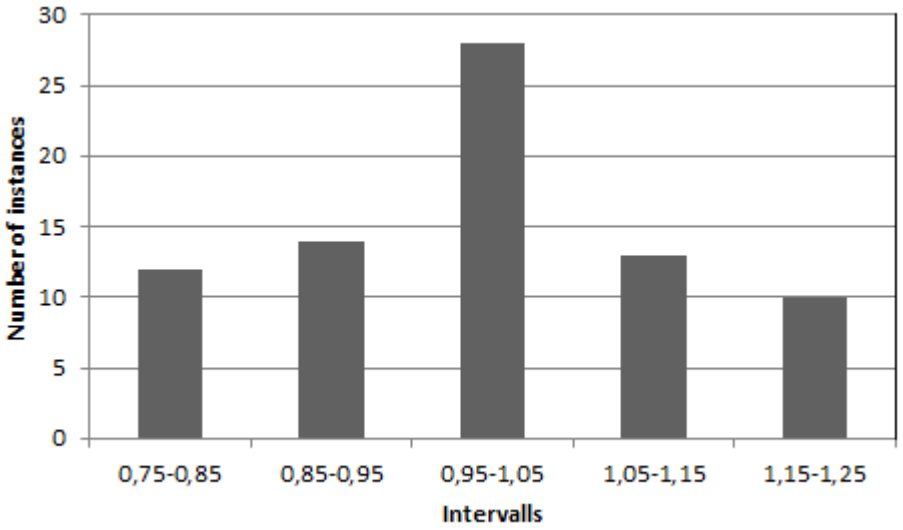

Figure 4.14. Calculated moisture content divided by measured moisture content

5 Conclusion

To assume that all drying air will become saturated before leaving the bed is wrong. The air that is in contact with bark all the time will most likely get saturated but some air will probably slip along the sides of the dryer. This leads to that the slip gets included in the heat transfer coefficient when optimizing towards the drying curve. Which leads to that the heat transfer coefficient from the optimization is probably higher in reality than the values calculated.

The drying rates for pine and birch were very well represented by the isotherm model. The for spruce it was not possible to get a good fit for the linear drying rate and at the same time a good representation at the declining drying rate at low moisture content. The fraction model dealt with this issue very well and a much better representation for the drying curve could be achieved.

The temperature profiles from the experiment always had an offset when compared to the model. The reason for this could be, as mentioned before, that some air travel along the sides of the dryer and get a much lower saturation of moisture and the air that goes through the middle actually would be saturated. This would lead to that the temperature would rise faster in the middle of the dryer, where the temperature is measured, and slower at the edges.

The fractions models distinct temperature plateaus do not represent the result from the experiments at all. These plateaus could be avoided by introducing a heat flux between the fractions, due to limited time this was excluded from the work. Also it is very hard to know what temperature that is actually measured from the experiments as the thermocouples was both surrounded by bark and air at different temperatures.

Bark types have different properties, such as density, heat transfer coefficients and moisture absorption properties.

6 Future work

Including heat transfer between fractions would give more realistic temperature profiles and shift them to the left as the heat flux overall would be larger. This is because the total heat flux through the small particles would be larger as some of the heat would be transferred through the small particles to the larger ones.

An alternative/complement to the fraction model would be a shrinking model, which would take the size reduction of particles over time into account. It has been noted during the experiments that the height difference before and after the drying have been around 10cm of the total height that was 67cm.

Air slip could be included as it could be possible that the air that goes through the bed and always have contact with the bed gets saturated. But if some air slips through this would decrease the average saturation which was modelled as no inner gradients were considered.

7 Table of abbreviations

Latin Symbol	Unit	Description
c	-	GAB parameter
Cp_a	kJ/kg°C	Heat capacity of air
Cp_b	kJ/kg°C	Heat capacity of bark
Cp_l	kJ/kg°C	Heat capacity of liquid water
Cp_v	kJ/kg°C	Heat capacity of water vapor
D_{eff}	m^2/s	Effective diffusion
d_p	m	Particle diameter
F_n	-	Bark fractions size
G	kg/s	Dry air flow
ΔH_{vap}	kJ/kg	Heat of water vaporization
ΔH_{sorp}	kJ/kg	Sorption energy of water in bark
ha	$kW/m^3°C$	Heat transfer coefficient
ha_n	$kW/m^3°C$	Heat transfer coefficient for bark fraction n
h	m	Height of volume element
k	-	GAB parameter
k_n	W/m°C	Heat conductivity
m	kg	Total bark mass
N_a	kg/s	Water vapor flux from bark to air
N_{an}	kg/s	Water vapor flux from bark fraction n to air
N_{at}	kg/s	Total water vapor flux from all bark fractions to air
P_{iso}	bar	Water vapor pressure at bark surface at low moisture content
P_{sat}	bar	Water vapor pressure of pure water
q	kW	Heat flux from air to bark

q_n	kW	Heat flux from air to bark fraction n
q_t	kW	Total heat flux from air to all bark fractions
r	m	Pipe radius
s_p	m^2	Particle surface area
T_a	°C	Air temperature
T_b	°C	Bark temperature
T_{bn}	°C	Bark fraction n temperature
Δt	s	Iteration time
u	kg water/kg dry matter	Bark moisture content
u_e	kg water/kg dry matter	Equlibrium bark moisture content
u_n	kg water/kg dry matter	Bark fraction n moisture content
V	m^3	Dryer volume
V_e	m^3	Dryer element volume
V_m	-	GAB parameter
V_p	m^3	Particle volume
v_0	m/s	Inlet air velocity
X_a	kg water/kg dry air	Moisture content in air
X_n	kg water/kg dry air	Moisture content in air at bark surface
X_o	kg water/kg dry air	Inlet air saturation
Greek Symbol		
σa	kg/m^3s	Mass transfer coefficient
σa_n	kg/m^3s	Mass transfer coefficient for bark fraction n
ε_b	-	Bulk porosity

ρ_a	kg/m^3	Air density
ρ_b	kg/m^3	Dry bark density
ρ_l	kg/m^3	Liquid water density
ρ_p	kg/m^3	Cellulose density
φ	-	Relative humidity

8 References

[1] H. Yang and M. R. Milota, "Modeling the Process of Drying Biomass in a Fixed Bed," *For. Prod. J.*, vol. 63, no. 5–6, pp. 148–154, Jun. 2013.

[2] J. Yrjölä and J. J. Saastamoinen, "Modelling and Practical Operation Results of a Dryer for Wood Chips," *Dry. Technol.*, vol. 20, no. 6, pp. 1077–1099, Jun. 2002.

[3] E. F. Zanoelo, G. M. di Celso, and G. Kaskantzis, "Drying Kinetics of Mate Leaves in a Packed Bed Dryer," *Biosyst. Eng.*, vol. 96, no. 4, pp. 487–494, Apr. 2007.

[4] P. Suvarnakuta, S. Devahastin, and A. S. Mujumdar, "A mathematical model for low-pressure superheated steam drying of a biomaterial," *Chem. Eng. Process. Process Intensif.*, vol. 46, no. 7, pp. 675–683, Jul. 2007.

[5] S.-E. Mörtstedt and G. Hellsten, *Data och Diagram*, 7th ed., vol. 7, no. 5. Liber AB, 2010, pp. 1–94.

[6] H. Holmberg and P. Ahtila, "Optimization of the bark drying process in combined heat and power production of pulp and paper mill," *Proc. 3rd Nord. Dry. Conf. …*, 2005.

[7] W. L. McCabe, J. C. Smith, and P. Harriott, *Unit Operations of Chemical Engineering*, 7th ed. McGraw-Hill, 2005.

[8] A. Martynenko, "The System of Correlations Between Moisture, Shrinkage, Density, and Porosity," *Dry. Technol.*, vol. 26, no. 12, pp. 1497–1500, Nov. 2008.

[9] A. Holmberg, L. Wadsö, and S. Stenström, "Water Vapour Sorption and Diffusivity in Bark," *Dry. Technol.*, no. 1, 2015.

[10] P. Lehtikangas, "Lagringshandbok för trädbränslen," *Uppsala Sveriges lantbruksuniversitet, Inst. för …*, pp. 1–116, 1999.

[11] S. Stenström, "Drying - Principles and process applications," in *Separation Processes, Advanced Course*, Lund, 2008, pp. 1–40.

[12] P. Heikkilä, "A Study on the Drying Process of Pigment Coated Paper Webs," Åbo Akademi.

9 Appendices

i. Spruce drying curves for the fraction model
ii. Birch drying curves for the fraction model
iii. Pine drying curves for the fraction model

i.

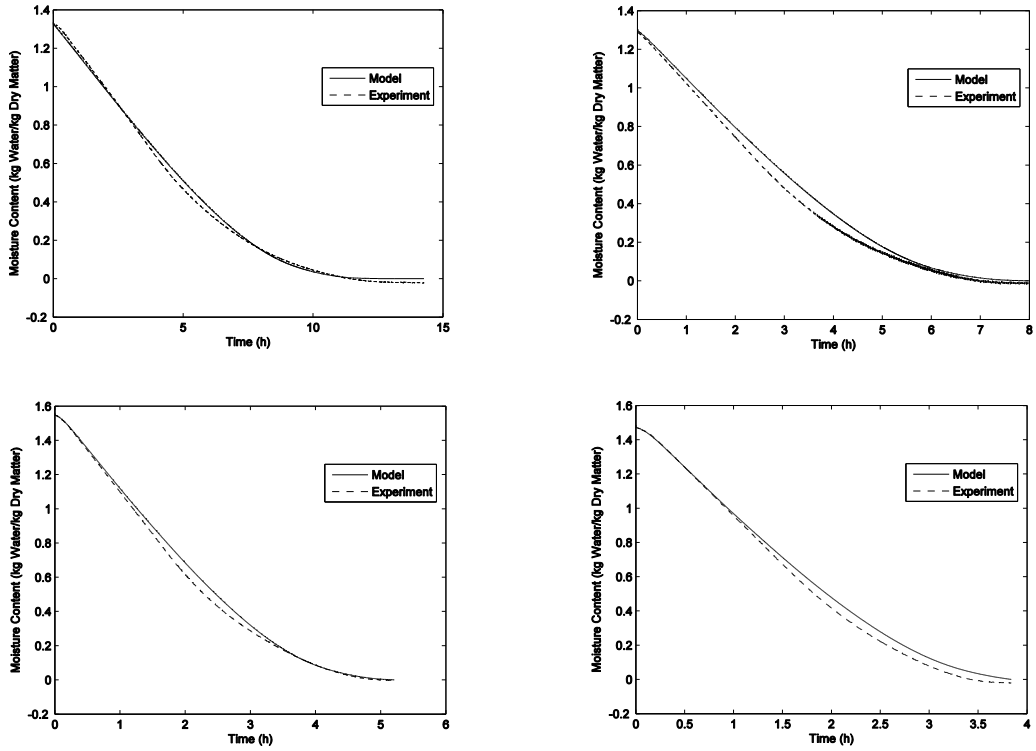

Drying rates for Spruce, in order 50, 70, 110 and 130 °C

ii.

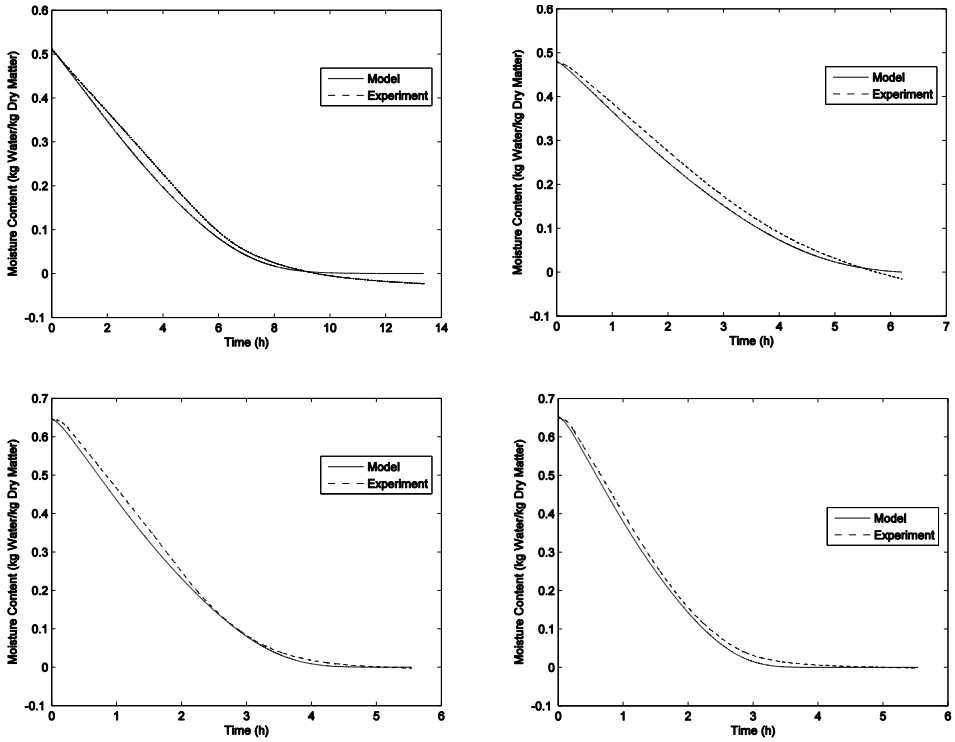

Drying rates for Birch, in order 50, 70, 110 and 130 °C

iii.

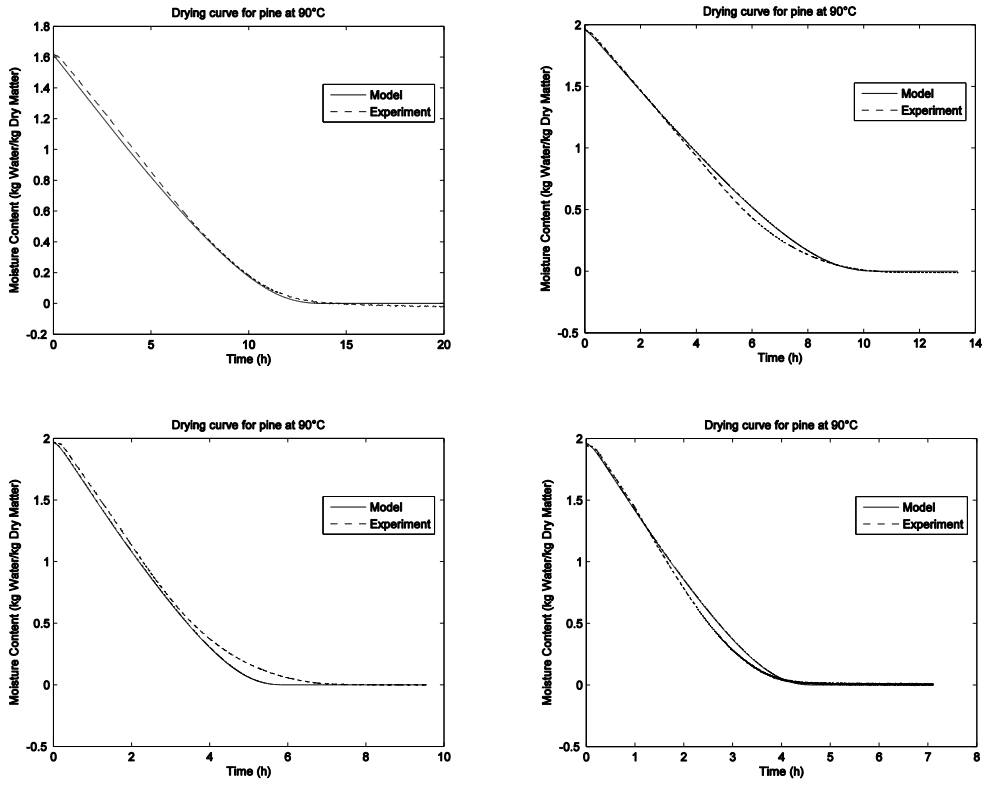

Drying rates for Pine, in order 50, 70, 110 and 130 °C